

スラブ脱水, 稍深発地震, 島弧マグマ活動
Slab dehydration, intermediate-depth earthquakes, and arc magmatism: A review of seismological observations

中島 淳一^{1*}

NAKAJIMA, Junichi^{1*}

¹ 東北大学大学院理学研究科

¹ RCPEV, Graduate School of Sci., Tohoku Univ.

We review recent seismological observations beneath the Japanese Islands and show important roles of geofluids on seismogenesis at intermediate depths and arc magmatism.

Seismicity in the subducting crust of cold slabs is most active at depths of 70-90 km, where seismic velocity in the crust abruptly increases, suggesting that high pore pressures generated as a result of dehydration reactions in the crust facilitate intermediate-depth seismicity. In contrast, seismicity is almost absent in the subducting crust of warm slabs like Cascadia and Nankai. The aseismic crust may be explained by slow dehydration rates in warm slabs, which cannot increase pore pressures effectively.

Magmatism beneath the arc has been discussed in terms of the heterogeneities in seismic velocities together with geochemical and petrological constraints. We recently developed simple but useful method to estimate seismic attenuation structures and applied it to waveform data in NE Japan. Seismic attenuation provides additional insights into ongoing magmatic processes in subduction zones, because higher-temperature environments or the existence of fluids may have different effects on seismic attenuation from on seismic velocity. The obtained results show that a depth profile of Q_p^{-1} in the back-arc mantle is explained by attenuation expected for a two-dimensional (2-D) thermal model. However, an inclined high-attenuation zone observed in the back-arc mantle wedge, which is interpreted as an upwelling flow, shows higher attenuation than that calculated from the 2-D thermal model. The higher seismic attenuation is probably caused by the concentration of partial melt in the upwelling flow. Our results further imply the breakdown of hydrous minerals in a hydrous layer above the Pacific plate at a depth of ~120 km.

Keywords: dehydration, pore pressure, eclogitization, seismic attenuation

Imaging mantle melting processes and the effect of water beneath island arcs and backarc spreading centers Imaging mantle melting processes and the effect of water beneath island arcs and backarc spreading centers

Wiens Douglas^{1*} ; WEI S. Shawn¹
WIENS, Douglas^{1*} ; WEI, S. shawn¹

¹Washington University, St Louis, MO, USA

¹Washington University, St Louis, MO, USA

We use arrays of land and ocean bottom seismographs to image melting processes in the Mariana and Tonga-Lau mantle wedges. Both regions show arc volcanism, active backarc spreading, and a gradient in mantle water content going from slab to backarc spreading center. The Lau backarc in particular shows a gradient in inferred mantle water content as the spreading centers approach the arc and slab in the south. Water contents range from near-MORB conditions in the Central Lau Spreading Center (CLSC) to high water content for the Eastern Lau Spreading Center (ELSC) and nearly arc-like for the Valu Fa Ridge (VFR).

For both Mariana and Lau we find significant slow velocity and high attenuation anomalies in the upper 100 km of the mantle beneath the volcanic arc and the spreading center. In the Mariana region, the anomalies are separated by a high velocity, low attenuation region at shallow depths (<80 km), implying distinct arc and backarc melting regions, with the anomalies coalescing and possibly allowing material interchange at greater depths. The maximum anomaly in the backarc is shallower (~30 km) than in the arc (~65 km), consistent with geochemical indications on the depth of melt production in these regions. The strongest anomaly beneath the backarc spreading center is narrow (~70 km) and extends from close to the mocho to 80 km depth. Data analyses for the Tonga-Lau project are preliminary, but show similarities to the Mariana images. Extremely low seismic velocity and high attenuation are found in a 100 km wide region beneath the spreading center in the upper 80 km. At deeper depths the anomaly is displaced westward in both velocity and attenuation images, suggesting that partial melting occurs along an upwelling limb of mantle flow originating west of the backarc. 3-D images from Rayleigh wave tomography show a much stronger anomaly along the CLSC when compared to the southern ELSC and VFR. The backarc velocity and attenuation anomalies are stronger in the Lau basin than in the Mariana backarc, perhaps due to higher mantle temperatures inferred from petrology.

Both Q and velocity anomalies are larger than expected for temperature effects based on laboratory-derived relationships, and their configuration is inconsistent with the expected temperature field. In addition, the observed anomalies are roughly inversely proportional to inferred mantle water content, suggesting that water content does not cause the observed large seismic anomalies. However, experimental results suggest that seismic attenuation and velocity are highly sensitive to the presence of even very small amounts of partial melt. Therefore we suggest the high attenuation and low velocity anomalies delineate the melt production regions beneath the ridge axis and volcanic arc, but that only small melt fractions (<1 %) are required to explain the seismic data. Smaller amplitude anomalies beneath the VFR, where large amounts of subduction-derived water are incorporated into the melt, may indicate lower mantle melt porosity due to low melt viscosity and more efficient transport of the water-rich melt, or a different topology of melt in the matrix. A lower melt porosity for aqueous melts is also consistent with the smaller seismic anomaly seen for the water-rich volcanic arc melting regions compared to the backarc melt production zone for both regions.

キーワード: seismic tomography, island arcs, backarc spreading centers, seismic attenuation, mantle fluids, melt generation
Keywords: seismic tomography, island arcs, backarc spreading centers, seismic attenuation, mantle fluids, melt generation

Slab Melting in Subduction Zones Slab Melting in Subduction Zones

SCHMIDT, Max^{1*} ; MANN, Ute¹
SCHMIDT, Max^{1*} ; MANN, Ute¹

¹ETH Zurich, Switzerland

¹ETH Zurich, Switzerland

Depending on temperature, slab-to-mantle element transfer in the subarc region may either occur through fluids or melts. In this contribution we present pelite melting experiments systematically varying H₂O and CO₂ contents and review the presently available information on slab melting. Synthetic pelite model compositions containing variable proportions of H₂O (0.7-4.4 wt%) and CO₂ (0-4 wt%) was melted at 3-4.5 GPa and 750-1200 °C. The fluid-saturation concentration at 3-8 GPa (i.e. the H₂O stored in phengite as the only hydrous phase) is 0.8-0.9 wt% H₂O. We locate the fluid-absent solidus of the H₂O-pelite system at 3 to 4.5 GPa at 880 °C to 1050 °C about 150-200 °C higher than the wet solidus (3 to 4.5 GPa, 730 to 860 °C). CO₂ increases the fluid-saturated solidus temperature by ~30 °C but leaves the fluid-absent solidus temperature unchanged. For all systems considered, the onset of melting is controlled by phengite and only in the fluid-absent experiments K-feldspar becomes a product of melting (at 3 GPa).

Compiling all available information, we parameterize the amount of melt to be formed as a function of temperature for fluid-saturated and fluid-undersaturated conditions. Melt compositions themselves are meta- to peraluminous high Si-granites (71-77 wt% SiO₂ on a volatile free basis) with low Fe, Mg, and Ca contents and are uniform to ~50% melting when plotted as a function of melt fraction (but not temperature), almost independent of starting compositions. At >2 wt% bulk H₂O melts are sodic (K/Na = 0.2-0.4), while at <1.5 wt% melts are mostly potassic (K/Na = 0.9-1.7). Only the fluid-poor H₂O-CO₂ and the CO₂-only experiments of Thomsen and Schmidt (2008, EPSL) and Tsuno and Dasgupta (2011, CMP) produce significantly different melts i.e. rather potassic phonolites (Na being increasingly retained in jadeitic cpx with pressure). Near 5 GPa a fundamental change occurs: the H₂O-silicate solidus comes to an endpoint while in CO₂-rich systems a carbonatite replaces the silicate melt lowering the solidus temperature by more than 100 °C to 9 GPa.

Regarding the likelihood of sediment melting in the subarc region, only the wet solidus is within reach of the hottest geotherms of the thermal models that predict the highest slab-surface temperatures, i.e. none of the Arcay et al (2007, EPSL) slab surface P-T paths cross the solidus while for Syracuse et al. (2010, G3) about 7 out of 56 modeled slab segments have P-T-paths that may lead to significant melting for H₂O-saturated pelites at 3-4 GPa. As retention of significant amounts of fluids within a subducting lithology is not an option, flushing with fluids from dehydrating serpentinites would be the only option for achieving significant melting in the hottest subduction zones (at the required P-T conditions, there are no suitable reactions in the mafic crust or the sediments themselves). An alternative option to reach widespread pelite melting would be to dismiss the rigid slab surface concept and allow for sediment diapirs to rise into the hot mantle (Gerya and Yuen, 2003, EPSL; Behn et al, 2011, Nature Geosci.) in which case the pelites could bleed out their incompatible elements completely. Nevertheless, these diapirs are propelled by a density contrast resulting from partial melting and it remains unclear whether they could start rising without melting in the first place.

In conclusion, combining P-T paths, phase diagrams and degrees of melting suggests that significant pelite melting at a rigid slab-mantle interface appears to be a rather rare on present day Earth (and hence much more so for mafic materials), the only option for widespread pelite melting appears to be entrainment of the sediments into the mantle wedge. Removal of CO₂ through melting is utterly inefficient and as subsolidus metamorphic reactions lead to low X_{CO2} fluids, most of the subducted CO₂ will be fed into the deep beyond-arc C-cycle.

キーワード: slab melting, H₂O, CO₂, pelite
Keywords: slab melting, H₂O, CO₂, pelite

西南日本における高温スラブ沈み込みによる様々なマグマの生成：フォワードモデルによる検討
Diverse magmatic effects of subducting a hot slab in SW Japan: results from forward modeling

木村 純一^{1*}; ギル ジェームズ²
KIMURA, Jun-ichi^{1*}; GILL, James²

¹ 海洋研究開発機構, ² カリフォルニア大学サンタクルツ校
¹JAMSTEC, ²University of California Santa Cruz

In response to the subduction of the young Shikoku Basin of the Philippine Sea Plate, arc magmas erupted in SW Japan throughout the late Cenozoic. Many magma types are present including ocean island basalt (OIB), shoshonite (SHO), arc-type alkali basalt (AB), typical sub-alkalic arc basalt (SAB), high-Mg andesite (HMA), and adakite (ADK). OIB erupted since the Japan Sea back-arc basin opened, whereas subsequent arc magmas accompanied subduction of the Shikoku Basin. However, there the origin of the magmas in relation to hot subduction is debated. Using new major and trace element and Sr-Nd-Pb-Hf isotope analyses of 324 lava samples from seven Quaternary volcanoes, we investigated the genetic conditions of the magma suites using a geochemical mass balance model, Arc Basalt Simulator version 4 (ABS4), that uses these data to solve for the parameters such as pressure/temperature of slab dehydration/melting and slab flux fraction, pressure, and temperature of mantle melting. The calculations suggest that those magmas originated from slab melts that induced flux-melting of mantle peridotite. The suites differ mostly in the mass fraction of slab melt flux, increasing from SHO through AB, SAB, HMA, to ADK. The pressure and temperature of mantle melting decreases in the same order. The suites differ secondarily in the ratio of altered oceanic crust to sediment in the source of the slab melt. The atypical suites associated with hot subduction result from unusually large mass fractions of slab melt and unusually cool mantle temperatures.

キーワード: 西南日本, 火山岩, 地球化学, フォワードモデル
Keywords: SW Japan, Volcanic rocks, Geochemistry, Forward model

日本沈み込み帯の流体と地震 Fluids and earthquakes in the Japan subduction zone

趙 大鵬^{1*}
ZHAO, Dapeng^{1*}

¹ 東北大学・理
¹Tohoku University, Department of Geophysics

Detailed tomographic images are determined for the source areas of large crustal and megathrust earthquakes that occurred in the Japan subduction zone during 1995-2013, thanks to the availability of the dense Japanese seismic network that could locate accurately the mainshocks and aftershocks of those large earthquakes and provide high-quality arrival-time data for tomographic imaging. Suboceanic events are relocated precisely using sP depth phase. Large crustal earthquakes in the forearc region such as the 1995 Kobe earthquake (M 7.2) and the 2011 Iwaki earthquake (M 7.0) might be triggered by fluids that are released from the dehydration of the subducting slab and directly ascend to the crust and enter an active fault zone. In contrast, along the volcanic front and in back-arc areas, the seismogenic layer in the upper crust is thinned and its mechanical strength is weakened because of ascending hot magmas and fluids which are produced by a combination of slab dehydration and corner flow in the mantle wedge. Large crustal earthquakes are apt to take place at the edge portion of the thinned seismogenic layer which exhibits low velocity, high Poisson's ratio, and high electrical conductivity. To clarify the generating mechanism of the 2011 Tohoku-oki earthquake (Mw 9.0) and the induced tsunami, we determined high-resolution tomographic images of the Northeast Japan forearc. Significant lateral variations of seismic velocity are visible in the megathrust zone, and most large interplate thrust earthquakes are found to occur in high-velocity (high-V) areas. These high-V zones may represent high-strength asperities at the plate interface where the subducting Pacific plate and the overriding Okhotsk plate are coupled strongly. A shallow high-V zone with large coseismic slip near the Japan Trench may account for the mainshock asperity of the 2011 Tohoku-oki earthquake. Because it is an isolated asperity surrounded by low-velocity patches, most stress on it was released in a short time and the plate interface became decoupled after the Mw 9.0 earthquake. Thus the overriding Okhotsk plate there was shot out toward the Japan Trench and caused the huge tsunami. Further details of the role of arc magma and fluids in the nucleation process of a large earthquake can be clarified by high-resolution geophysical imaging and multidisciplinary studies of the earthquake fault zones.

References

- Huang, Z., D. Zhao (2013) Relocating the 2011 Tohoku-oki earthquakes (M 6.0-9.0). *Tectonophysics* 586, 35-45.
- Huang, Z., D. Zhao (2013) Mechanism of the 2011 Tohoku-oki earthquake (Mw 9.0) and tsunami: Insight from seismic tomography. *J. Asian Earth Sci.* 70, 160-168.
- Tong, P., D. Zhao, D. Yang (2012) Tomography of the 2011 Iwaki earthquake (M 7.0) and Fukushima nuclear power plant area. *Solid Earth* 3, 43-51.
- Zhao, D., H. Kanamori, H. Negishi, D. Wiens (1996) Tomography of the source area of the 1995 Kobe earthquake: Evidence for fluids at the hypocenter? *Science* 274, 1891-1894.
- Zhao, D., O. Mishra, R. Sanda (2002) Influence of fluids and magma on earthquakes: seismological evidence. *Phys. Earth Planet. Inter.* 132, 249-267.
- Zhao, D., M. Santosh, A. Yamada (2010) Dissecting large earthquakes in Japan: Role of arc magma and fluids. *Island Arc* 19, 4-16.
- Zhao, D. et al. (2011) Structural heterogeneity in the megathrust zone and mechanism of the 2011 Tohoku-oki earthquake (Mw 9.0). *Geophys. Res. Lett.* 38, L17308.

キーワード: 流体, 地震, 日本列島, 沈み込み帯, マグマ, スラブ
Keywords: fluids, earthquakes, Japan Islands, subduction zones, magma, slab

Silicate solute in aqueous fluids governs trace element and stable isotope behavior in subduction zones

Mysen Bjorn^{1*}
MYSEN, Bjorn^{1*}

¹Geophysical Laboratory, CIW, USA

¹Geophysical Laboratory, CIW, USA

Physical and chemical properties of fluids equilibrated with subducting deep crust and overlying upper mantle are saturated in silicate components [1]. These components govern physical and chemical properties of the fluids. For example, the solution behavior of volatile components such as hydrogen, carbon, and nitrogen, which form bonding with silicate components in fluids, will differ from the behavior in pure H₂O fluids [2]. This can also affect isotope fractionation between fluids and condensed silicate materials.

In pure H₂O, hydrogen bonding plays a role to temperatures <600 °C at pressures in the 1 GPa-range with a ΔH for hydrogen bond formation near 20 kJ/mol. At temperatures less than 600 °C, physical properties of fluids, including density, compressibility, and viscosity, are non-linear functions of temperature, whereas at higher temperature and in the absence of hydrogen bonding, these properties tend to become linear functions of temperature. Solution of silicate components in aqueous fluids changes these relationship. The silica solubility in equilibrium with quartz/coesite reaches >5 mol/kg near 5 GPa and 900 °C with polymerized silicate species, SiO₄, Si₂O₇, and SiO₃ in the fluid. In equilibrium with enstatite and forsterite, the silicate solubility is ~50% less and only SiO₄ and Si₂O₇ species exist in the fluids. Those variables affect D/H isotope ratios. For example, the fluid/melt partition coefficients for hydrogen, KH, varies by ~40% as a function of variable silicate speciation in fluids in the 500 °C-800 °C/0.5-1 GPa temperature and pressure range. The hydrogen fluid/melt partition coefficient exceeds that of deuterium. Their temperature-dependence also differs so that for the exchange equilibrium of D and H between coexisting water-saturated melt and silicate-saturated aqueous fluid, the ΔH is between -4 and -6 kJ/mol. This difference is because in the more silicate-rich fluids (higher proportion of polymerized silicate species), the abundance ratio, OD/OH, is higher in the more polymerized silicate species in the fluid. As a result, increasing pressure, which leads to increasingly polymerization of silicate, will cause the D/H ratio of the fluid will increase. This also means that D/H fractionation between aqueous fluid and condensed silicate increases with increasing pressure.

Interaction between dissolved silicate components and other elements can also affect their solubility and, therefore, their roles as geochemical tracers. For example, in the system rutile+H₂O, the Ti solubility in the few-GPa-range at ~1000 °C is on the order of 1-100 ppm as compared with thousands of ppm in silicate-saturated aqueous solution [3]. This difference between pure H₂O and silicate-saturated fluid is related to interaction with the silicate species dissolved in the fluid, 2M₆Si₂O₇ + 4H₂O + TiO₂ = 4(MH)₂SiO₄ + M₄TiO₄, where M is a metal cation. Similar situation likely exist for other nominally insoluble, highly charged elements (e.g., Al³⁺, Zr⁴⁺, Hf⁴⁺, P⁵⁺).

When modeling isotope fractionation and partitioning of nominally insoluble elements between fluid and condensed phases (melts and minerals) in the deep crust and upper mantle of the Earth, the silicate solute concentration and structure in the fluid and the water concentration and structure of silicate melts both can have major effects on the fractionation factors. These factors depend on the element or isotope ratio in question. They also vary with pressure (and likely temperature) because the structure of dissolved silicate in aqueous fluids varies with pressure and temperature.

[1] C. E. Manning, *Eart Planet. Sci. Lett.* 2004, 223, 1-16.

[2] B. O. Mysen, *Lithos* 2012, 148, 228-246.

[3] A. Antignano and C. E. Manning, *Chemical Geology* 2008, 255, 283-293.

キーワード: aqueous fluid, solubility, subduction, stable isotope, structure, fluid property

Keywords: aqueous fluid, solubility, subduction, stable isotope, structure, fluid property

D/H intramolecular partitioning in alkali silicate melts: with implications for tracing subduction processes

D/H intramolecular partitioning in alkali silicate melts: with implications for tracing subduction processes

LE LOSQ, Charles^{1*}; CODY, George¹; MYSEN, Bjorn¹
LE LOSQ, Charles^{1*}; CODY, George¹; MYSEN, Bjorn¹

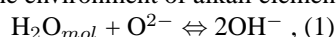
¹Geophysical Laboratory, Carnegie Institution of Washington

¹Geophysical Laboratory, Carnegie Institution of Washington

The D/H ratio is an important probe for studying the cycle of water in the Earth interior in general, and in subduction zones in particular. Indeed, D/H ratios in melt inclusions (MIs) of arc magmas for instance indicate that the δD of subduction fluids is high, near -30 ‰, compared to the δD of the mantle that is near -80 ‰. A possible explanation for these different values is that D/H fractionation during dehydration of the slab in subduction zones enriches the subduction fluids in D, leading to high δD values in subduction magmas. This might be accomplished with hydrogen exchange between the melt and another source enriched in D before entrapment of MIs or a diffusive loss of H from within the inclusion leading to D/H fractionation. However, chemical effects affecting the δD ratio have not been considered because it is usually assumed that D and H have the same chemical and structural properties in silicate melts and glasses.

However, recent results from ²H and ¹H MAS NMR of Na₂Si₄O₉ glasses quenched from melt (equilibrated with fluid at 1400°C and 1.5 GPa) with various amounts of (D_xH_(1-x))₂O (x = D/[D+H]) lead to the conclusion that D and H isotopes occupy different structural positions in the network. From the ¹H MAS NMR spectra OH⁻ groups are distributed in two environments with mean O ··· O distances close to 0.26 and 0.29 nm in the Na₂Si₄O₉ glass. These environments give rise to two strong NMR lines at 16 and 5 ppm respectively. By contrary, ²H MAS NMR spectra of the same glasses display a strong line at 16 ppm accompanied by a small band near 5 ppm regardless of D/H ratio and total water concentration. This observation leads to the suggestion that OD⁻ groups are mainly present in an environment with small O ··· O distances. In other words, the structural behavior of OH⁻ and OD⁻ groups in the quenched silicate melts (glasses) differs.

In M₂Si₄O₉ glasses, (M = Li, Na or K) with different concentrations of pure H₂O or D₂O (from 3.3 up to 17.6 mol%), ²H and ¹H MAS NMR spectra confirm that by exchanging H with D the intensity of the 16 ppm NMR line increases greatly, whereas the intensity of the 5 ppm line decreases drastically. Interestingly, such a spectral evolution is also observed when increasing the size of the alkali element in the network of hydrous alkali silicate glass. These effects are attributed to steric and electronic effects in the environment of alkali elements, which cause shifts in the equilibrium between H₂O the O²⁻ of the silicate network:



The specific preference of OD⁻ groups for small O ··· O sites is in this mind intriguing, but is not in conflict with previous observations. Indeed, increasing the ionic size of alkali elements lead to promote OH⁻ in the small O ··· O environment. Similarly, it appears that increasing the size of the proton (by substituting H by D) promotes their existence in this small O ··· O environment. On this basis, we propose that those two observations have a common origin, maybe related to the probability of interaction between H/D and alkali elements depending of their ionic size and/or to molar volume effects related to those ionic sizes.

This large structural-controlled partitioning of D and H in melts, which depends on the melt composition, might be another fractionation process affecting the δD of subduction melts. Consequently, δD values recorded in MIs might be the result of such a structural process and might not reflect the δD of released fluids in the mantle wedge during slab subduction.

キーワード: D/H isotopes, silicate glass, NMR spectroscopy, Raman spectroscopy, Subduction fluids

Keywords: D/H isotopes, silicate glass, NMR spectroscopy, Raman spectroscopy, Subduction fluids

Speciation and solubility of F and Cl in coexisting fluids and silicate melts: implications for F and Cl signature in arc
Speciation and solubility of F and Cl in coexisting fluids and silicate melts: implications for F and Cl signature in arc

DALOU, Celia^{1*}; MYSEN, Bjorn²; FOUSTOUKOS, Dionysis²
DALOU, Celia^{1*}; MYSEN, Bjorn²; FOUSTOUKOS, Dionysis²

¹Jackson School of Geosciences, The University of Texas at Austin, ²Geophysical Laboratory, Carnegie Institution of Washington

¹Jackson School of Geosciences, The University of Texas at Austin, ²Geophysical Laboratory, Carnegie Institution of Washington

The effect of pressure and temperature on the structure of silicate melts coexisting with silica-saturated aqueous electrolyte solutions enriched in fluorine or chlorine in the Na₂O-Al₂O₃-SiO₂-H₂O system has been determined. In-situ measurements were conducted with the samples at desired temperatures and pressures in a hydrothermal diamond anvil cell (HDAC) by using microRaman and FTIR spectroscopy techniques. The data were acquired at high temperature and pressure (up to 800°C and 1264 MPa, respectively), and during cooling/decompression to ambient conditions.

The intensity of the Raman bands assigned to stretch vibration of the OH-groups relative to those of coexisting molecular H₂O in silicate melts is lower in the presence of F and Cl. This difference reflects the interaction of F or Cl with H₂O in the melts. With decreasing pressure and temperature (P-T) conditions, SiF complexes are favored in the melt rather than in the fluid, perhaps because of decreasing silicate concentration in fluids with decreasing temperature and pressure. In melts, the solubility of Cl, likely in the form of NaCl_(aq), increases with decreasing P-T conditions, whereas the abundance of such complexes in coexisting fluids decreases.

Our experimental data were employed to help model the ascent of a magma-fluid system from the upper mantle to the shallow crust. The information offers particular insights into F and Cl partitioning between and the speciation of F and Cl in melts and magmatic fluids. We suggest that the formation of stable SiF and NaCl complexes and their increasing solubilities during magma ascent explain the late volcanic degassing of F and Cl, compared to other volatile species.

It explains why F and Cl are often undersaturated in arc basaltic magmas (Carroll and Webster, 1994), indicating that they often do not significantly experience a degassing event. In contrast to H₂O, CO₂ and S, F and Cl signature in primary arc magmas (arc melt inclusions) can be considered as primary and likely retain information on arc magma sources.

Those results also imply that, while Cl is enriched in aqueous fluids from slab dehydration, F preferentially dissolves in slab melts or supercritical fluids, during flows from the subducted slab into the zone of melting in the mantle wedge. It is therefore expected that at given pressure and temperature, the Cl/F ratio is significantly lower in slab melt and supercritical fluids, than in aqueous fluids. This difference in Cl/F signatures decreases when slab components are dragged down to the deep mantle.

キーワード: Fluorine, Chlorine, silicate melt, aqueous fluid, speciation, HDAC
Keywords: Fluorine, Chlorine, silicate melt, aqueous fluid, speciation, HDAC

The Structure of Water-Saturated Carbonate Melts The Structure of Water-Saturated Carbonate Melts

FOUSTOUKOS, Dionysis^{1*}; MYSEN, Bjorn O.¹
FOUSTOUKOS, Dionysis^{1*}; MYSEN, Bjorn O.¹

¹Geophysical Laboratory, Carnegie Institution of Washington, USA

¹Geophysical Laboratory, Carnegie Institution of Washington, USA

The structure of water-saturated Ca- and Mg-bearing carbonate melts under reducing and oxidizing conditions was investigated in a series of hydrothermal anvil cell experiments conducted at 400 - 1100 °C and 442 - 2839 MPa. Equilibria were investigated in the calcite-H₂O, calcite-CaO-H₂O, magnesite-H₂O and magnesite-MgO-H₂O systems, with redox conditions controlled by Re/ReO₂ and Ti/TiO₂ assemblages. Melting relationships and the C-O-H speciation of the coexisting aqueous fluid and melt were assessed in-situ by Raman vibrational spectroscopy. Hydrous melting of MgCO₃-MgO occurred at ~850 °C, 1.5 - 2 GPa. In the CaCO₃-CaO-H₂O system, melt was formed at 600 - 900 °C and pressures of 0.5 - 1.5 GPa because of melting-point depression imposed by the presence of CaO. The C-O-H speciation of the carbonate melts and coexisting supercritical aqueous solutions was mainly H₂O and CO₃²⁻, with traces of CO_{2(aq)} and CH_{4(aq)} in the fluid phase. The melt-fluid H₂O partition coefficients attained in the Mg-bearing melt (median 0.5) were higher than in the Ca-bearing melt (median 0.3). Under oxidizing redox conditions, dissolved ReO⁴⁻ was present in all phases, underscoring the enhanced solubility of trace elements and metals in carbonate-bearing melts and carbonatites. In effect, the enhanced solubility of H₂O along with the ionic nature of the carbonate melts may promote the solvation of ionic species in the melt structure.

From in-situ vibrational spectroscopy, the ν_1 -CO₃²⁻ vibration recorded in the melt spectra suggests the presence of intermolecular interactions between the oxygen of the carbonate ion with water dissolved in the melt. The thermodynamic properties of this water appear to be similar to the supercritical aqueous phase. For example, the estimated enthalpy for the breakage of the hydrogen bonding between water molecules attained values of 6.8 ± 1.5 kcal/mol and 8.4 ± 1.3 kcal/mol in the melt and fluid phase, respectively. The calculated partial molar volume of H₂O in the melt ($\sim 48 \pm 6$ cm³/mol) is also comparable to the partial molar volume of supercritical water at similar conditions. Interestingly, this value is considerably greater than published partial molar volume values for H₂O in silicate melts (10-12 cm³/mol).

The pressure-temperature melting relationships of the CaO-CO₂-H₂O and MgO-CO₂-H₂O systems highlight the important role of water and alkali earth oxides on the hydrous melting of the carbonate-bearing subducting oceanic crust. Carbonates present in marine sediments or serpentinized peridotites may melt before complete dehydration at the slab-mantle wedge transition zone, and thus, never reach sub-arc depths. To this end, melting of carbonate minerals at crustal temperatures and pressure can contribute to the volcanic CO₂ flux at the arc through melt/fluid interactions.

キーワード: carbonate melt, aqueous solutions, hydrothermal diamond anvil cell, raman vibrational spectroscopy
Keywords: carbonate melt, aqueous solutions, hydrothermal diamond anvil cell, raman vibrational spectroscopy

北海道で観測されるスラブ内地震の後続波と海洋性地殻の構造 (その2) Later phase observations and seismic velocity structure in the subducting crust of the Pacific slab beneath Hokkaido

椎名 高裕^{1*}; 中島 淳一¹; 豊国 源知¹; 松澤 暢¹; 北 佐枝子²

SHIINA, Takahiro^{1*}; NAKAJIMA, Junichi¹; TOYOKUNI, Genti¹; MATSUZAWA, Toru¹; KITA, Saeko²

¹ 東北大・理・予知セ, ² 防災科研

¹ RCPEV, Grad. Sch. of Sci., Tohoku Univ., ² NIED

海洋プレートの沈み込みに伴い地球内部に供給された水は、沈み込み帯における地震活動や島弧マグマ活動と密接に関係していると考えられている (e.g., Kirby et al., 1996; Nakajima et al., 2013). 特にスラブ最上部に存在し、地震波速度の遅い海洋性地殻は含水鉱物として多量の水を保持しており、これらの鉱物の脱水反応や相転移の進行が海洋性地殻の地震波速度やスラブ内の水の分布に影響していると考えられている (e.g., Hacker et al., 2003). したがって、海洋性地殻の詳細な構造を明らかにすることは、沈み込み帯における水循環やスラブ内地震の発生メカニズムを理解する上で非常に重要である。

しかしながら、海洋性地殻の厚さは 7 km 程度であり、初動走時解析などの従来の手法では、地殻の構造不均質を詳細に推定することは困難である。一方で、スラブ内地震で観測される後続波 (PS 変換波や guided wave など) は海洋性地殻やスラブマントルを長い距離伝播するため、スラブの構造不均質により敏感であることが知られている (e.g., Matsuzawa et al., 1986; Abers, 2005)。

本研究では、北海道の日高山脈西部で観測される後続波 (e.g., 清水・前田, 1980) を解析し、北海道東部下に沈み込む海洋性地殻の地震波速度を推定することを試みる。本研究で注目する後続波は、P 波初動の 2-10 秒後に P 波初動よりも大きな振幅を持つ波群として観測される。椎名・他 (2013, 地震学会) ではフォワードモデリングにより後続波の伝播過程を検討し、海洋性地殻内を伝播する guided P-wave であると再解釈した。本解析では彼らの解釈に基づき、guided P-wave の同定と走時の読み取りを行い、海洋性地殻の P 波速度を推定した。加えて、guided P-wave が観測される観測点とイベントのペアに対して、初動 S 波の理論走時より数秒遅れて S 波的な振動を持つ振幅の大きな波群が到着することが確認された。この波群 (Xs phase) に対してもフォワードモデリングにより伝播過程を検討し、観測される走時などを guided P-wave と比較した結果、Xs phase は海洋性地殻内を S 波として伝播した波群、すなわち guided S-wave として解釈できることがわかった。

P 波と S 波、それぞれに対応する guided wave は、地震波速度の遅い海洋性地殻内部を伝播し、海洋性地殻と日高山脈下でスラブ直上まで分布する低速度域 (大陸地殻物質; Kita et al., 2010, 2012) の接触により地表へ放出されると考えられる。このため、同一観測点で観測された guided wave の走時差をとることで、イベント間の海洋性地殻の地震波速度を見積もることができる。本研究では北海道日高山脈西部で観測された太平洋スラブ内地震の観測波形記録から guided wave の読み取りを行い、それぞれ guided P-wave で 117 個、guided S-wave で 56 個の走時から海洋性地殻の地震波速度を推定した。その結果、北海道東部下に沈み込む海洋性地殻に対して、深さ 50-100 km 程度の範囲で、P 波で 6.8-7.7 km/s、S 波で 3.5-4.0 km/s の速度が得られた。深さ 100 km 以浅で得られた P 波速度は東北地方下で推定された海洋性地殻の P 波速度 (Shiina et al., 2013) と同様に、MORB などの含水鉱物から期待される P 波速度 (約 7.2 km/s) よりも小さい。このことは北海道東部下でも海洋性地殻内で流体の水と含水鉱物が共存して存在している可能性を示している。一方で、海洋性地殻の S 波速度に関しては、読み取った走時のデータ数も十分でなく、読み取りの精度も P 波に比べて低いという問題がある。このため、今後、guided wave の読み取りを増やすなどして、S 波速度の推定精度向上させる必要がある。

キーワード: 海洋性地殻, 後続波, guided wave, 太平洋スラブ

Keywords: subducting crust, later phase, guided wave, the Pacific slab

Pore fluid geochemistry and carbonates in cores and cuttings from the Nankai accretionary prism

Pore fluid geochemistry and carbonates in cores and cuttings from the Nankai accretionary prism

EVEN, Emilie^{1*}; SAMPLE, James C.²; FUCHIDA, Shigeshi¹; IODP EXPEDITION 348, Shipboard scientists³
EVEN, Emilie^{1*}; SAMPLE, James C.²; FUCHIDA, Shigeshi¹; IODP EXPEDITION 348, Shipboard scientists³

¹Graduate School of Science, Osaka City University, ²School of Earth Sciences and Environmental Sustainability, Northern Arizona University, ³IODP Expedition 348

¹Graduate School of Science, Osaka City University, ²School of Earth Sciences and Environmental Sustainability, Northern Arizona University, ³IODP Expedition 348

The recent IODP Exp 348 at Site C0002 has successfully deepened Hole C0002F (Exp 338) down to 3058.5 mbsf, deep into the accretionary prism of the Nankai Trough. During Exp 348, cuttings were collected and analysed from drilled interval of Holes C0002N (875 mbsf- 2325 mbsf) and C0002P (1965 mbsf- 3059 bsf) and limited coring was performed from 2163 to 2218 mbsf in Hole C0002P. The major-element composition of the solid cuttings and the geochemistry of interstitial water in cores was determined. Results provide insights into exchange of elements between minerals and pore water phases, and into geochemical signatures related to lithological changes within the prism. This study reports the main geochemical results from IODP Exp 348.

Interstitial waters were collected using the GRIND method (Wheat et al., 1994), in which core sediments were ground in an agate mill with ultra-pure water. The interstitial water percentage was determined by drying sediments at 60 °C and 105 °C, the former to minimize loss of clay-bound water, and the latter to follow the GRIND procedure used in previous expeditions. Concentrations were interpreted with data corrected for dilution at 60 °C, 105 °C and normalised to chlorinity values. Profiles of carbonates (as CaCO₃), organic carbon and total nitrogen were determined from cuttings of 1-4 mm and >4 mm sizes and are compared with the observed lithological boundaries. Carbonate veins were observed in a core sample exhibiting a fault zone at 2205 mbsf, but no increase was observed at the same depth in the carbonates profile.

The GRIND method has limitations in recovering absolute values of dissolved ions in interstitial waters, and yielded very high dissolved-ion concentrations in some samples. But comparison of ions normalized to chlorinity yielded results comparable to what was observed in pore waters at shallower depths of Site C0002. Some of the trend variations in the cuttings profiles of carbonates, organic carbon and nitrogen match the unit boundaries determined by observation of lithological changes in the cuttings. Therefore, it can be suggested to integrate these data when defining geological units.

Wheat, Boulegue and Mottl (1994) Proc. ODP, Sci. Results, 139: College Station, TX (Ocean Drilling Program), 429-437

キーワード: Accretionary prism, GRIND method, IODP Expedition 348, Nankai Trough, Pore water

Keywords: Accretionary prism, GRIND method, IODP Expedition 348, Nankai Trough, Pore water

Solution mechanism of water in depolymerized silicate melts Solution mechanism of water in depolymerized silicate melts

Chertkova Nadezda^{1*}; 山下 茂¹
CHERTKOVA, Nadezda^{1*}; YAMASHITA, Shigeru¹

¹Okayama University, ISEI

¹Okayama University, ISEI

It is known that the effect of dissolved water on the viscosity of silicate melts is larger for polymerized melts than for depolymerized melts [e.g., 1, 2]. Direct spectroscopic measurements of melt structure and water speciation at high temperature provide information about the mechanism of water dissolution and its influence on the physical properties of the melts. While *in situ* measurements of water speciation were widely conducted for rhyolitic melts and their analogues [e.g., 3, 4, 5], only limited data are available for depolymerized silicate melts.

We performed high-temperature near-infrared and Raman spectroscopic measurements of hydrous Na₂Si₂O₅ melts (2.3-8.1wt% H₂O) using externally heated diamond anvil cell (HDAC). Na₂Si₂O₅ composition was chosen as a structural analogue of basaltic melt (anhydrous NBO/T = 1). Experimental pressure was monitored with the pressure- and temperature-dependent Raman shift of ¹³C diamond [6]. Near-infrared spectra of the homogeneous liquid phase, observed above 820 degree C, 1.7GPa in the Na₂Si₂O₅+2.3wt%H₂O system and above 700 degree C, 1.6GPa in the Na₂Si₂O₅+8.1wt%H₂O system, contain absorption peaks corresponding to molecular H₂O (at ~5200 cm⁻¹) and structurally bound OH groups (at ~4500 cm⁻¹). At 900 degree C and 1.6-1.9GPa the ratio of these peaks height remains approximately constant (2.6-2.2), implying a constant (structurally bound OH)/(molecular H₂O) ratio for this range of water contents. This observation differs from the regularities reported for more polymerized melts (rapid decrease of OH/H₂O with total water content) [e.g., 4, 7]. At the same time no pressure effect on the ratio of 4500 cm⁻¹ peak height to 5200 cm⁻¹ peak was observed below 2.4 GPa.

References

- [1] Whittington A., Richet P., Holtz F. (2000) *Geochim Cosmochim Acta* 64, 3725-3736.
- [2] Giordano D., Russell J.K., Dingwell D.B. (2008) *Earth. Planet. Sci. Lett.* 271, 123-134.
- [3] Sowerby J.R., Keppler H. (1999) *Am. Mineral.* 84, 1843-1849.
- [4] Nowak M., Behrens H. (2001) *Earth. Planet. Sci. Lett.* 184, 515-522.
- [5] Shen A.H., Keppler H. (1995) *Am. Mineral.* 80, 1335-1338.
- [6] Mysen B.O., Yamashita S. (2010) *Geochim. Cosmochim. Acta* 74, 4577-4588.
- [6] Mysen B.O. (2010) *Geochim. Cosmochim. Acta* 74, 4123-4139.
- [7] Botcharnikov R.E., Behrens H., Holtz F. (2006) *Chem. Geol.* 229, 125-143.

キーワード: water speciation, hydrothermal diamond anvil cell, near-infrared spectroscopy, Raman spectroscopy
Keywords: water speciation, hydrothermal diamond anvil cell, near-infrared spectroscopy, Raman spectroscopy